arXiv:0809.0873v1 [physics.bio-ph] 4 Sep 2008

Sequence-specific size, structure, and stability of tight protein knots

Joachim Dzubiella

*Physics Department T37, Technical University Munich, 85748 Garching, Germany**

Abstract

Approximately 1% of the known protein structures display knotted configurations in their native fold but their function is not understood. It has been speculated that the entanglement may inhibit mechanical protein unfolding or transport, e.g., as in cellular threading or translocation processes through narrow biological pores. Protein knot manipulation has become accessible in single molecule experiments, e.g., leading to knot tightening and localization. Here we investigate *tight* peptide knot (TPK) characteristics in detail by pulling selected 3_1 and 4_1-knotted peptides using all-atom molecular dynamics computer simulations. We find that the 3_1 and 4_1-TPK lengths are typically $\Delta l \simeq 4.7$ nm and 6.9 nm, respectively, for a wide range of tensions ($F \lesssim 1.5$ nN), pointing to a pore diameter of $\simeq 2$ nm below which a translocated knotted protein might get stuck. The 4_1-knot length is in agreement with recent AFM pulling experiments. Detailed TPK characteristics however, may be *sequence-specific*: we find a different size and structural behavior in polyglycines, and, strikingly, a strong hydrogen bonding and water molecule trapping capability of hydrophobic TPKs due to side chain shielding of the polar TPK core. Water capturing and release is found to be controllable by the tightening force in a few cases. These mechanisms result into a sequence-specific 'locking' and metastability of TPKs what might lead to a blocking of knotted peptide transport at designated sequence-positions. Intriguingly, macroscopic tight 4_1-knot structures are reproduced microscopically ('figure-of-eight' vs. the 'pretzel') and can be tuned by sequence in contrast to mathematical predictions. Our findings may explain a function of knots in native proteins, challenge previous studies on macromolecular knots, and may find use in bio- and nanotechnology.

Keywords: protein knot, molecular dynamics simulation, AFM pulling, buried water, side-chain shielding, hydrogen bonds

*To whom correspondence should be addressed. E-mail: jdzubiel@ph.tum.de

I. INTRODUCTION

After the discovery of the first knotted structure in the native fold of a protein in 1994 [1], additional studies [2, 3], and in particular a recent survey identified almost three hundreds of further knotted proteins, constituting around 1% of known structures in the protein data base [4]. Most of them have the simplest 3_1 (trefoil) topology, only a few have been found to posses the more complicated 4_1 (figure-eight) and 5_2-types of prime knots. While the question of physiological relevance is still a matter of debate [3, 5, 6] it has been proposed that the entangled structure might have profound effects on protein folding and (forced or mechanical) unfolding [4, 6, 7, 8], e.g., to inhibit translocation through biological membranes or to protect against degradation by proteasome threading. In this respect it is tempting to speculate that the steric blocking of narrow pathways by a localized or tightly pulled protein knot may have bio(techno)logical significance. Also relevant, cyclotides, a family of proteins that have a cyclic peptide backbone, strong biological activity, and high pharmaceutical potential, feature a tightly packed cystine knot in their interior [9]. The synthesis and design of artificially interlocked molecules has become possible in supramolecular chemistry with applications in bio- or nanotechnology, e.g., as molecular receptors, locks, or machines [10, 11].

The study of tight knot characteristics in (bio)polymers has a long history of interest as knots easily self-tie and localize in any long chain [12, 13, 14, 15]. More than 20 years ago de Gennes argued that knots may self-tie in crystallizing or sheared polymer melts changing their macroscopic relaxation behavior [16]. Possible self-tying mechanisms may be based on electrostatic repulsion [17], entropic tightening in worm-like chains [18], or localization of (flat) polymer knots either in confinement [19, 20, 21] or in bad solvent conditions [13]. Externally controlled manipulation and characterization of microscopic knots has become accessible experimentally by employing optical tweezer methods [22, 23], or atomic force microscopy (AFM) [6, 24]. From a theoretical perspective, scaling arguments [18], (water-free) quantum calculations [25], or coarse computer simulations [13, 26, 27, 28, 29, 30] have been used. Almost exclusively, previous studies focused on homogeneous systems such as polyethylene, DNA, or actin filaments; only recently tight protein knots (TPKs) with specific, inhomogeneous sequences have been investigated by Sułkowska *et al.* using an (implicit solvent) Go-model [31]. Due to local geometry (e.g., side chain size or kinks in the peptide) and in strong contrast to previous findings [17, 23, 29, 30, 32] knot localization and diffusion was dominated by jumps of the knot's ends to specific peptide locations suggesting qualitatively different, sequence-dependent fluctuations of TPKs when compared to homopolymers.

Although highly relevant for transport, translocation, and threading processes of knotted proteins the size of a TPK has not been determined before. For an educated guess, consider a rope of (contour) length l_c, tie a knot in it and pull it tight. The end-to-end distance l is now reduced by $\Delta l = l_c - l$ which we refer to in the following as the *tight knot length*, i.e., the length of the rope involved in the 'open' knot [33]. By dividing Δl by the rope thickness D, we obtain the characteristic quantity [34]

$$\Lambda = \frac{\Delta l}{D} \tag{1}$$

which is minimized by the tight knot conformation, and is Λ=10.1 and 13.7 for a 3_1 and 4_1, respectively, for idealized hard-core ropes [34]. Assuming now a typical peptide thickness of

the order of an atomic size, $D \simeq 0.35 - 0.5$ nm, we expect $\Delta l = \Lambda D \simeq 3.5 - 5.1$ nm and $\simeq 4.8 - 6.9$ nm for tight 3_1 and 4_1 peptide knots, respectively. If, naively, the knot is further assumed to be a circle with diameter $\Delta l = 2\pi R$ we infer that a typical TPK radius may be of $R \simeq 0.6 - 1.1$ nm.

In this work, we take a more detailed look at TPKs by performing *explicit-water* molecular dynamics (MD) computer simulations [35] of 3_1 and 4_1-knots in selected polypeptides involving up to 30 amino acids and systematically study their size and structural behavior. We find tight knot lengths $\Delta l \simeq 4.7 \pm 0.3$ nm (involving 13 ± 1 amino acids) and $\simeq 6.9 \pm 0.3$ nm (19 ± 1 amino acids) for the 3_1 and 4_1, respectively, surprisingly constant for a wide range of stretching forces ($F \lesssim 1.5$ nN), and typical tight knot radii of gyration of $R_g \simeq 0.7 - 0.8$ nm, all in the range of the macroscopic estimate (1). The 4_1-TPK length is in agreement with recent AFM pulling experiments on the natively knotted bacterial phytochrome [36]. Detailed tight knot characteristics however, may be sequence specific, e.g., we find smaller knots, and different structural and stability behavior in the special case of polyglycines. Strikingly, TPKs have a strong water capturing and hydrogen bonding capability within their closely packed interior, which is sequence-specific and promoted by nonpolar side-chains. Buried water and long-lived intra-knot hydrogen bonds lead to surprisingly rigid and stable tight knots in free simulations on a ~ 100 ns time scale. Intriguingly, macroscopic tight 4_1-knot structures are reproduced microscopically ('figure-of-eight' vs. a 'pretzel'-like configuration) but depend on peptide sequence in contrast to mathematical predictions of the tight 4_1-knot structure which is the 'figure-of-eight' figure [34]. We predict strongly localized tight knots after peptide stretching and a preferential affinity towards regions with dominantly nonpolar side chains. We demonstrate that the accurate modeling of specific side chains *and* the aqueous environment is crucial for the full understanding of TPK characteristics.

II. METHODS AND SYSTEMS

A. MD simulations

Our all-atom MD simulations are performed using the software package Amber9.0 with the ff03 force-field and TIP3P solvent [37]. Systems are maintained at a fixed pressure of $P = 1$ bar and temperature $T = 300$ K by coupling to a Berendsen barostat and Langevin thermostat, respectively. System sizes vary between $N \simeq 4000$ and $N \simeq 8000$ atoms. Electrostatic neutrality is assured by additional Na^+-counterions compensating the net peptide charge given at pH=7. The rectangular and periodically repeated simulation box has edge lengths $L_x \simeq L_y \simeq 30$ Å, while in peptide stretching direction $L_z \simeq 5.5 - 7.0$ Å. Electrostatic interactions are calculated by particle mesh Ewald summation and real-space interactions have a cut-off of 9 Å. Polypeptides are generated using the Amber *tleap* tool. Knots are tied into them utilizing interactive MD (IMD) in VMD [38]: while a Langevin simulation of the peptide is running and visualized a force can be applied to selected fragments by using the computer mouse so that the peptide can be dragged by hand into a finally knotted configuration. Thereafter, the system is equilibrated for $\simeq 5$ ns with Langevin dynamics, solvated with TIP3P water, and further equilibrated by a $\simeq 5$ ns MD simulation. For peptide stretching and loosening we utilize the Amber steered MD (SMD) tool: a constant pulling velocity of 0.1 Å/ns (0.01 m/s) drives the first and last atom (in a distance l) of the peptide backbone in opposite directions and force-extension curves $F(l)$ are calculated. Pulling is terminated after the mean force reaches $\sim$1.5 nN, a value at which covalent bond breaking can occur

experimentally [24]. Simulation snapshots are generated using VMD [38]. Hydrogen bonds, radii of gyration, and rms deviations are analyzed using the Amber *ptraj* tool.

B. Systems

3_1 and 4_1-types of knots are investigated. To study the influence of amino acid type on the tight knot structure we opt for three different homopeptides: the hydrophobic polyleucine (sequence $\mathrm{L}_{N_{\mathrm{aa}}}$), the partly hydrophilic and charged polyglutamic acid ($\mathrm{E}_{N_{\mathrm{aa}}}$), and the slim, amphiphilic polyglycine ($\mathrm{G}_{N_{\mathrm{aa}}}$). The peptides have a total number of N_{aa}=21 and 30 amino acids for the 3_1 and 4_1-knots, respectively. Furthermore, two randomly picked pieces from the knotted cores of the natively 3_1-knotted YibK methyltransferase [39] and the 4_1-knotted Class II ketol-acid reductoisomerase [40] are considered to directly connect to naturally occurring protein knots. In the following we name the knotted peptides by knot type and sequence, e.g., '3_1L' for a polyleucine trefoil and '4_1mix' for the 4_1-knot in a mixed sequence. The different knotted peptide systems, their amino acid (aa) sequences and numbers N_{aa} are summarized in Tab. I.

III. RESULTS AND DISCUSSION

A. Tight knot size and structure

A typical initial configuration of a 3_1-knotted peptide in our simulation is shown in Fig. 1 a) where a snapshot of 3_1G is sketched before pulling it tight. The end-to-end extension here is $l \simeq 25$Å. A tight knot situation for the same peptide is shown in Fig. 1 b) for a large stretching force of ∼1.5 nN ($l \simeq 45$Å). For an elastic peptide as considered in this study the final 'tightness' of the knot will naturally depend on the external stretching force F. The calculated force-extension curve, $F(l)$, for 3_1G is shown in Fig. 2 a) together with the data for 3_1E and 4_1L. We observe an overall monotonic nonlinear increase of the force. Fluctuations are moderate on that scale and have local standard deviations ranging from ~ 20 pN up to ~ 50 pN. Note that we also plot $F(l)$ of knot loosening, i.e., 'reverse pulling', showing no obvious hysteresis. This indicates that our systems are close to equilibrium at the chosen pulling rate of 0.1 Å/ns.

In order to determine the tight knot length $\Delta l(F) = l_c(F) - l(F)$ an accurate estimate for the force-dependent contour length $l_c(F)$ of the unknotted peptide is needed. For this, we calculate the average amino acid length $\Delta l_{\mathrm{aa}}(F)$ by measuring the mean distance between neighboring backbone nitrogen atoms in short unknotted peptides, presented in the inset to Fig. 2 a): below a stretching force of around ∼10 pN the length thermally fluctuates around $\Delta l_{\mathrm{aa}}(F) \simeq 3.5$ Å, then rises quickly with force in a nonlinear fashion in the low-stretching, thermal regime ($F \sim 10$ - 150 pN) to eventually increase linearly in the high stretching regime $F \gtrsim 150$ pN. At $F = 1.5$ nN a value of $\Delta l_{\mathrm{aa}}(F) \simeq 3.8$ Å is reached. From the slope b of the linear part we estimate the linear elastic modulus $\Gamma = \Delta l_{\mathrm{aa}}(F = 0)/b \simeq 42$ nN, which is in agreement with AFM pulling experiments, where $\Gamma \simeq 50 \pm 15$ nN [41]. This agreement is remarkable since MD force-fields are typically not benchmarked to be accurate at considered large tensions.

In pulling experiments, rupture of some terminal bonds at the AFM tip can occur at forces of around F_1 =200 pN [24], where we find $\Delta l_{\mathrm{aa}}(F_1) \simeq 3.68$ Å, leading to contour

length estimates $l_c(F_1) = N_{\rm aa}\Delta l_{\rm aa} \simeq 77.3$ Å and $l_c(F_1) \simeq 110.4$ Å for the trefoil and the 4_1 peptides, respectively. Consequently, it follows that the tight knot lengths for the trefoil peptides are between $\Delta l(F_1) \simeq 44.3$ Å (3_1G) and $\simeq 49.8$ Å (3_1L). The number of amino acids involved in the knot are thus $n_{\rm aa} = \Delta l/\Delta l_{\rm aa} \simeq 13$. For the 4_1-knots three of the four values lie between $\Delta l \simeq 68.4$ Å and 71.9 Å ($n_{\rm aa} \simeq 19$) while for the polyglycine knot (4_1G) we find $\Delta l(F_1) \simeq 60.4$ Å ($n_{\rm aa} \simeq 13$), around 14% smaller. The lengths are summarized in Tab. I. A typical error of these values is given by the fluctuations of the $F(l)$ curve and is roughly of amino acid size (±3 Å).

Let us know consider more intense stretching and study the knot lengths at a larger force $F_2 = 1$ nN. $\Delta l_{\rm aa}(F)$ increases to $\simeq 3.76$ Å giving rise to a slightly larger contour length for the unknotted peptides. Evaluating the particular knot lengths we observe that the knots shrink in size (while the whole peptide is more stretched) as could have been anticipated. Although the pulling force is substantially increased typically only one amino acid less is involved in a single knot, so that surprisingly the knot sizes vary only a few percent for a wide range of tensions. An exception however, are both of the polyglycine peptides: here the tightening effect is considerable and the final knot lengths are 20-25% smaller than those of the other studied peptides. All lengths are summarized in Tab. I.

The knot lengths of $\simeq 4.7$ nm and $\simeq 6.9$ nm for the 3_1 and 4_1-knots, respectively, fall inside the range of prediction (1) indicating on a first glance that they are primarily determined by *generic* packing effects with an effective excluded volume thickness D similar for most of the peptides. Furthermore, macroscopic arguments roughly hold on the molecular scale. In contrast, hydrophobicity and hydrophilicity seem to have no direct influence on tight knot size in the considered force regime. Examining a bit closer the nature of the amino acid side chains supports this statement: while the glycine side chain is identical to just a single hydrogen atom, a typical residue with a few carbon atoms gives rise to a more difficult molecular arrangement close to or inside the tight knot. This presumably leads to the 20-25% smaller knots in the special case of polyglycine. For the latter we thus find a smaller effective thickness $D \simeq 3.7$ Å, while for the other peptides $D \simeq 4.6 - 5.0$ Å. Importantly, apart from the polyglycine, all 4_1-TPK lengths are in agreement with recent AFM pulling experiments on the natively knotted bacterial phytochrome [36].

Illustrating simulation snapshots are shown in Fig. 3 where we plot tight knot situations for the peptides 4_1G and 4_1mix including their side chains. Large side chains obviously impede tight peptide packing. We also calculate the radius of gyration R_g of the knots, i.e., by averaging root mean square (rms) atomic distances from the geometric center of the atoms involved in the knot, i.e., constituting the length Δl. We measure $R_g \simeq 7.2 \pm 0.2$ Å and $R_g \simeq 7.8 \pm 0.2$ Å for the 3_1 and 4_1 knots, respectively, with only weak dependence on the stretching force for all considered peptides apart from the polyglycine. For the latter radii of gyration are found to be close to the values above for weak stretching ($F \sim 200$ pN) but 20% smaller for strong stretching ($F \gtrsim 1$ nN). These TPK sizes are larger or comparable as the size of biological channels such as in the protease [8, 42] so that a translocation of a knotted protein would indeed be blocked by the presence of a knot.

An intriguing topological feature appears when inspecting the overall 4_1-knot structure without the obscuring side chains, as in Fig. 1 c) and d). While the 4_1G knot is figuratively indeed in a figure-eight configuration 4_1L displays a 'pretzel'-like configuration. Actually, we find that *all* the considered 4_1-knots expect from 4_1G prefer the pretzel when inspected by eye. This comes as a surprise as the tight 4_1-knot configuration which minimizes (1) has been shown to be figuratively the 'figure-of-eight', at least using simplifying mathematical

assumptions [34]. Presumably the reasons are rather physics-based, i.e., high friction or lowering of the system free energy due more favorable amino acid interactions and packing around the knot region may result into the pretzel. Interestingly, the pretzel-like configuration can be a stable 4_1-configuration in macroscopic knots under tension, e.g., as can be easily self-demonstrated using a simple computer cable, or as taught in books on cowboy rope tricks, see Fig. 4.

B. Water trapping, hysteresis, and hydrogen bonding

A striking structural feature we observe is the capability of some peptide knots to capture and strongly bind water molecules in their interior. The simulated peptides show this effect with varying magnitude, i.e., we find no bound water in polyglycine (3_1G and 4_1G) and the mixed peptide 3_1mix for any simulated peptide extension, while in 3_1E a single trapped water molecule is reproducibly found only in the case of very close peptide packing at high forces $F \gtrsim 1$ nN. We find stronger water binding qualities for the other four peptides 3_1L, 4_1E, 4_1L, 4_1mix for a wider range of simulated peptide extensions, i.e., water was bound for simulation times of the order of ∼10-100 ns per peptide pointing to a quite stable mechanism. On a first glance surprisingly, both homopeptides with the purely hydrophobic leucine side chains show the strongest water trapping capability.

Simulation snapshots are shown in Fig. 5 for the peptides 4_1E and 4_1mix: the water bonds to the backbone amides in the knot interior, involving at least three hydrogen bonds per molecule, and is rotationally immobilized. Apparently the water binding is made possible by the tight peptide packing in the highly bent knot allowing for multiple bonds of a water molecule to the polar backbone. A particularly interesting case is the water binding in 3_1L. Here the bound water molecule is *squeezed out* of the knot interior for large stretching forces $F \simeq 1$ nN. This behavior leads to a strong force peak in the force extension curve as shown in Fig. 2 b): for extensions $l \lesssim 30$ Å the water molecule is bound as shown in the left snapshot. At $l \simeq 30$ Å and $F \simeq 1$ nN the bound water is 'wrung' out and the force drops significantly before further increasing. When the knot is loosened $F(l)$ shows a considerable hysteresis. However, a water molecule is captured by the knot again during loosening at extensions $l \lesssim 27$ Å and $F \simeq 200$ pN. Repeating the stretching-loosening loop twice shows *quantitative reproducibility* of this effect [cf. Fig. 2 b)]. The occurrence of the hysteresis points to the fact that the water binding-unbinding events fluctuate on large time-scales and this simulation deviates therefore from equilibrium. The magnitude of the hysteresis can be estimated by integrating over the $F(l)$ stretching-loosening cycle which gives rise to a large dissipation energy of about $\Delta G \simeq 30 - 35\ k_{\mathrm{B}}T$, indeed comparable to the energy of 3-4 hydrogen bonds between a water molecule and a peptide environment (8-10 $k_{\mathrm{B}}T$ per hydrogen bond) [43].

It is a well-known fact that buried water molecules constitute an integral part of many native protein structures contributing to stability, flexibility, folding, and mechanical and enzymatic function [44, 45, 46, 47]. Noteworthy, our measured ΔG is very close the binding enthalpy of a buried water molecule in the polar pocket of bovine pancreatic trypsin inhibitor (BPTI) [48], where four hydrogen-bonds constitute $\Delta H \simeq 36\ k_{\mathrm{B}}T$. We find a similar large dissipation energy in peptide 4_1mix ($\Delta G \simeq 20 k_B T$) and less pronounced in 4_1E ($\Delta G \simeq 12 k_B T$) and 3_1E ($\Delta G \simeq 5 k_B T$) due to partial water hydrogen binding events during knot tightening. No hysteresis is found in 4_1L as water is bound here during the full stretching-loosening loop without any binding/unbinding transition.

Interestingly, in the sequence 3_1mix we find no water trapped in the knot interior for all peptide extension in contrast to 4_1mix, where we observe water bound on a $\sim$ 10 ns time scale with three binding/unbinding events for tension $F \lesssim 500$ pN. A closer inspection of the MD trajectory reveals that the immediate surrounding of the buried water molecule consists of 6 amino acids, ALD FQS, which create a mostly hydrophobic environment, see Fig. 5 b). This observation and the strong water binding capabilities of the polyleucines indicate that nonpolar side chain environments promote water hydrogen bonding to the tightly packed polar backbone. We explain this by the textbook-fact that hydrogen bonds are generally stronger in a nonpolar and/or *desolvated* protein environment [43, 49], where electrostatic interactions are only weakly screened. We suspect that additionally the hydrophobic side chains impose a large energy barrier for a possible escape of a water molecule. In the polyglutamic acids water screening and the (probably lower) barrier is likely to be provided by the methylene groups of the side chains immediately surrounding the knotted peptide region. A nonpolar environment is clearly absent in the polyglycines. However, strong water trapping capability seems to results from a unique and delicate combination of local backbone structure and a specific, but rather nonpolar amino acid side chain environment.

Related to this, another consequence of the tight peptide packing as further revealed by our simulations is the existence of long-lived hydrogen bonds between particular backbone amide groups. For instance during the $\simeq$ 200 ns stretching and loosening loop of polyleucine 4_1L we find that amino acids 10 and 24 hydrogen bond for $\simeq 80\%$ of the simulation time. Detailed analysis yields similar behavior for the other peptides, i.e., intrapeptide hydrogen bonds are stable on a long $\sim$10-100 ns time scale. An exception is polyglycine, where the longest hydrogen bond life expectancy is found to be one or two orders of magnitude shorter.

C. Free simulations and tight knot stability

We also conduct free simulations of the knotted peptides without any constraints in order to check whether the knots dissolve on a typical simulation time scale. Initial configurations are taken from a stretched situation with $F \simeq 200$ pN. Dissolution of a knot is loosely defined here by connecting the peptide ends with an imaginary line and looking whether we find a knot in the closed loop or not. Only both of the polyglycine knots, 3_1G and 4_1G, show strong fluctuations and unknot quickly on a time scale of $\sim$10 ns. All other investigated knots do *not* dissolve in a $\simeq$ 120 ns simulation pointing to a (meta)stable tight knot situation. For quantifying this we measure the rms deviation from the initial structure and find values of $\sim$ 2 Å increasing quickly within $\sim$ 10 ns to $\simeq$ 7 Å for the polyglycines. For the other peptides however, the rms value stays at $\simeq$ 2 Å for the total simulation time, supporting the observation that apart from the polyglycines tight knots stay stable and quite rigid after peptide stretching on relatively long time scales. We note that dissolution of the polyglycine proceeds rather via a knot 'swelling' than a 'slithering' mechanism (where the knot stays tight and diffuses to the end), possibly to relax the highly bent backbone. This needs not to be in contrast to study [18] where an entropic tightening and slithering was predicted as this might be the dominant mechanism for somewhat 'looser' tight knots.

As in the constrained case closer inspection of the knot structure reveals a few long-lived hydrogen bonds in all stable knots. A representative illustration is shown in Fig. 5 c) where we plot a MD snapshot of 4_1mix after a $\simeq$ 120 ns free simulation. Four hydrogen bonds are found between amide backbone groups right at the knot's ends clearly inhibiting the opening of the knot. Typically, we find that these hydrogen bonds persist on average $\simeq$ 100 ns (80-

90%) of the total free simulation time, even slightly longer for the polyleucines. In 3_1mix (where no buried water could be detected) the longest hydrogen-bond life time is shorter ($\simeq$ 50-60 ns). Remarkably, in 3_1L and 4_1L additionally one water molecule was trapped during the full, unconstrained simulation, constituting a remarkable total of 7-8 long-lived hydrogen bonds within the knots. Again the high quantity and persistence strength of hydrogen bonds in 3_1L and 4_1L must be attributed to the desolvated, strongly nonpolar side chain environment of the tight knot.

IV. CONCLUDING REMARKS

In summary, our MD study of TPKs have revealed some generic, but also unexpectedly specific behavior and provoke some interesting speculations and future prospects:

As previously conjectured, the steric blocking of narrow pathways by a localized or tightly pulled knot might be possible *in vivo* and also relevant for biotechnological purposes. In this light interesting are our findings that TPKs exhibit an unexpectedly strong stability and their radii of gyration are all indeed slightly bigger ($\sim$7-8 Å) at moderate stretching ($F \lesssim 200$ pN) than the radius of the protease pore ($\sim$6.5 Å) [8, 42]. We predict that a translocated knotted protein should get stuck in pores with a diameter below $\simeq 2$ nm.

Interesting for further investigation not only from a topological point of view [50] is the observation that most 4_1-knots are figuratively not in a figure-eight but rather in a 'pretzel'-like configuration, which might be a (meta)stable configuration in 'physical' open tight knots in contrast to those underlying simplifying mathematical assumptions [34]. The pretzel may be stuck by high molecular friction, e.g., caused by hydrogen bonds, and/or preferred by the lowering of the system free energy due to favorable amino acid arrangements.

As a striking result we find that the TPK interior has a strong water binding and hydrogen bonding capability which is promoted in rather nonpolar side-chain environments. These mechanisms result in 'locking' of the knot structure and surprisingly stable and rigid tight knots after peptide stretching in unconstrained MD simulations on a $\sim$ 100 ns time scale. The observed *quantitative* reproducibility of squeezing-out and capturing a water molecule at well-defined tensions may allow for an external *mechanical control* of the capturing and releasing of single water molecules by designed peptide knots. Important in this respect is that buried water is known to be an integral part of native protein structures and not only affects protein flexibility and folding [45, 46, 48] but can be essential for catalytic action [47].

Furthermore, TPKs might resemble structural elements of the cyclotide protein family – constituted by short ($\sim$ 30 aa) cyclic peptides with a tight cystine knot – which has strong potential in drug design [9]. In view of their structural complexity and close relation to native phenomena (engineered) TPKs thus might serve as an important model system for a deeper understanding of protein folding and stability [51], and enzymatic activity, and may be useful for pharmaceutical purposes due to a possible catalytic function.

Finally, we would like to encourage further experiments in this stimulating field which are readily available using AFM [36] or optical tweezer methods [22, 23]. Desirable are studies on protein knot length and size, stability, and diffusion behavior along stretched peptides and the refolding of knotted proteins after stretching. Particularly interesting is knotted peptide translocation for probing the mechanical forces involved in protein unfolding, knot tightening and blocking, e.g., by threading them through narrow biological or solid-state nanopores [52]. Buried water molecules in peptide knots might be detectable by nuclear magnetic relaxation dispersion methods (NMRD) [45] allowing for another experimental

method to explore TPK fluctuations and energy landscapes.

Acknowledgments

J. D. is grateful to Thomas Bornschlögl, Katrina Forest, and Matthias Rief for pointing to this interesting project, Lyderic Bocquet, Ralf Metzler, Roland Netz, and Joachim Seel for useful comments, and the Deutsche Forschungsgemeinschaft (DFG) for support within the Emmy-Noether-Program. Computing time on the HLRBII computer cluster of the Leibniz-Rechenzentrum München is acknowledged.

---

1. Mansfield, M. L. 1994. Are there knots in proteins? *Nat. Struct. Biol.* 1:213.
2. Taylor, W. R., and K. Lin. 2003. A tangled problem. *Nature*. 421:25.
3. Lua, R. C., and A. Y. Grosberg. 2006. Statistics of knots, geometry of conformations, and evolution of proteins. *PLOS Computational Biology*. 2:350.
4. Virnau, P., L. A. Mirny, and M. Kardar. 2006. Inricate knots in proteins: function and evolution. *PLOS Computational Biology*. 2:1074.
5. Taylor, W. R. 2007. Protein knots and fold complexity: some new twists. *Comp. Biol. Chem.* 31:151.
6. Alam, M. T., T. Yamada, U. Carlsson, and A. Ikai. 2002. The importance of being knotted: effects of the c-terminal knot structure on enzymatic and mechanical properties of bovine carbonic anhydrase II. *FEBS Letters*. 519:35.
7. Wallin, S., K. B. Zeldovich, and E. I. Shakhnovich. 2007. The folding mechanics of a knotted protein. *J. Mol. Biol.* 368:884.
8. Prakash, S., and S. Matouschek. 2004. Protein unfolding in the cell. *Trends Biochem. Sci.* 29:593–600.
9. Rosengren, K. J., N. L. Daly, M. R. Plan, C. Waine, and D. J. Craik. 2002. Twists, knots, and rings in proteins - structural definition of the cyclotide framwork. *J. Biol. Chem.* 278:8606–8616.
10. Breault, G. A., C. A. Hunter, and P. C. Mayers. 1999. Supramolecular topology. *Tetrahedron*. 55:5265.
11. Williams, A. R., B. H. Northrop, T. Chang, J. F. Stoddart, A. J. P. White, and D. J. Williams. 2006. Suitanes. *Angew. Chemie. Int. Ed.* 40:6665.
12. Belmonte, A. 2007. The tangled web of self-tying knots. *Proc. Natl. Acad. Sci.* 104:17243–17244.
13. Virnau, P., V. Kantor, and M. Kardar. 2005. Knots in globule and coil phases of a model polyethylene. *JACS*. 127:15102.
14. Kardar, M. 2007. The elusiveness of polymer knots. *EPJ B*. Topical issue Stat. Phys. 23, Genova.
15. Katritch, V., W. K. Olson, A. Vologodskii, J. Dubochet, and A. Stasiak. 2000. Tightness of random knotting. *Phys. Rev. E*. 61:5545.
16. de Gennes, P.-G. 1984. Tight knots. *Macromolecules*. 17:703.
17. Dommersnes, P. G., Y. Kantor, and M. Kardar. 2002. Knots in charged polymers. *Phys. Rev. E*. 66:031802.

18. Grosberg, A. Y., and Y. Rabin. 2007. Metastable tight knots in a worm-like polymer. *Phys. Rev. Lett.* 99:217801.
19. Metzler, R., A. Hanke, P. G. Dommersnes, Y. Kantor, and M. Kardar. 2002. Equilibrium shapes of flat knots. *Phys. Rev. Lett.* 88:188101.
20. Ercolini, E., F. Valle, J. Adamcik, G. Witz, R. Metzler, P. D. L. Rios, J. Roca, and G. Dietler. 2007. Fractal dimension and localization of dna knots. *Phys. Rev. Lett.* 98:058102.
21. Marcone, B., E. Orlandini, and A. L. Stella. 2007. Knot localization in adsorbing polymer rings. *Phys. Rev. E.* 76:051804.
22. Arai et al., Y. 1999. Tying a molecular knot with optical tweezers. *Nature.* 399:446.
23. Bao, X. R., H. J. Lee, and S. R. Quake. 2003. Behavior of complex knots in single dna molecules. *Phys. Rev. Lett.* 91:265506.
24. Hugel, T., and M. Seitz. 2001. The study of molecular interactions by afm force spectroscopy. *Macromolecular Rapid Communication.* 22:989–1016.
25. Saitta, A. M., P. D. Soper, E. Wasserman, and M. L. Klein. 1999. Influence of a knot on the strength of a polymer strand. *Nature.* 399:46.
26. Mansfield, M. L. 1997. Tight knots in polymers. *Macromolecules.* 31:4030.
27. Farago, O., Y. Kantor, and M. Kardar. 2002. Pulling knotted polymers. *Europhys. Lett.* 60:53.
28. Arteca, G. A. 2007. Externally steered relaxation of tight polyethylene tangles with different initial knot topologies. *Theor. Chem. Account.* 118:549.
29. Vologodskii, A. 2006. Brownian dynamics simulation of knot diffusion along a stretched dna molecule. *Biophys. J.* 90:1594–1597.
30. Huang, L., and D. E. Makarov. 2007. Langevin dynamics simulations of the diffusion of molecular knots in tensioned polymer chains. *J. Phys. Chem. A.* 111:103338.
31. Sułkowska, J. I., P. Sułkowski, P. Szymczak, and M. Cieplak. 2008. Tightening of knots in proteins. *Phys. Rev. Lett.* 100:058106.
32. Metzler, R., W. Reisner, R. Riehn, R. Austin, J. O. Tegenfeldt, and I. M. Sokolov. 2006. Diffusion mechanisms of localised knots along a polymer. *Europhys. Lett.* 76:696.
33. Mathematically these knots are open, i.e., no closed loops, but throughout the work we just use the term 'knot' for simplicity.
34. Pierański, P., S. Przybyl, and A. Stasiak. 2001. Tight open knots. *E. Phys. J. E.* 6:123–128.
35. Karplus, M., and J. A. McCammon. 2002. Molecular dynamics simulations of macromolecules: A perspective. *Nat. Struct. Mol. Biol.* 9:646–652.
36. Bornschlögl, T., D. Anstrom, J. Dzubiella, M. Rief, and K. T. Forest. 2008. Tightening the phytochrome knot by single molecule atomic force microscopy. Submitted.
37. Case, D. A. 2006. Software AMBER9.0, University of California, San Francisco.
38. Humphrey, W., A. Dalke, and K. Schulten. 1996. *J. Molec. Graphics.* 14:33.
39. Lim, K., H. Zhang, A. Tempczyk, W. Krajewski, N. Bonander, and J. Toedt. 2003. Structure of the yibk methyltransferase from haemophilus influenzae (hi0766): A cofactor bound at a site formed by a knot. *Proteins Struct. Funct. Genet.* 51:56–67.
40. Biou, V. et al. 1997. The crystal structure of plant acetohydroxy acid isomeroreductase complexed with nadph, two magnesium ions and a herbicidal transition state analog determined at 1.65 å resolution. *EMBO J.* 16:3405–3415.
41. Ptak, A., S. Takeda, C. Nakamura, J. M. M. Kageshima, S. P. Jarvis, and H. Tokumoto. 2001. Modified atomic force microscope applied to the measurement of elastic modulus for a single peptide molecule. *J. Appl. Phys.* 90:3095.
42. Pickart, C. M., and A. P. VanDemark. 2000. Opening doors into the proteasome. *Nat. Struct.*

Mol. Bio. 7:999–1001.
43. Jackson, M. B. 2006. Molecular and Cellular Biophysics. Cambridge University Press.
44. Baker, E. N. New York. Solvent interactions with proteins as revealed by X-ray crystallographic studies. M. Dekker, 1995. In Protein-Solvent Interactions (R.B. Gregroy, ed) 143-189.
45. Denisov, V. P., J. Peters, H. D. Hörlein, and B. Halle. 1996. Using buried water molecules to explore the energy landscape of proteins. *Nat. Struc. Biol.* 3:505–509.
46. Dougan, L., G. F. H. Lu, and J. M. Fernandez. 2008. Solvent molecules bridge the mechanical unfolding transition state of a protein. *Proc. Natl. Acad. Sci.* 105:3185.
47. Ball, P. 2008. Water as an active constituent in cell biology. *Chem. Rev.* 108:74–108.
48. Fischer, S., and C. S. Verma. 1999. Binding of buried structural water increases the flexibility of proteins. *Proc. Natl. Acad. Sci.* 96:9613–9615.
49. Roseman, M. A. 1988. Hydrophobicity of the peptide c=oh—n hydrogen-bonded group. *J. Mol. Biol.* 201:621–623.
50. Katritch, V., J. Bednar, D. Michoud, R. G. Scharein, J. Dubochet, and A. Stasiak. 1996. Geometry and physics of knots. *Nature.* 384:142–145.
51. Yeates, T., T. S. Norcross, and N. P. King. 2007. Knotted and topologically complex proteins as models for studying folding and stability. *Curr. Opinion Chem. Biol.* 11:595.
52. Dekker, C. 2007. Solid-state nanopores. *Nature Nanotechnology.* 2:209–215.
53. Mason, B. S. 1928. How to Spin a Rope: Lariat Throwing, Rope Spinning and Trick Cowboy Knots. Self published, Columbus, OH.

Knot	aa-sequence	$N_{\rm aa}$	$l_{\rm c}(F_1)$/Å	$l(F_1)$/Å	$\Delta l(F_1)$/Å	$n_{\rm aa}(F_1)$	$l_{\rm c}(F_2)$/Å	$l(F_2)$/Å	$\Delta l(F_2)$/Å	$n_{\rm aa}(F_2)$
3_1L	L_{21}	21	77.3	27.5	49.8	14	79.0	32.5	46.5	12
3_1E	E_{21}	21	77.3	31.0	46.3	12	79.0	32.5	46.5	12
3_1G	G_{21}	21	77.3	33.0	44.3	12	79.0	42.0	37.0	10
3_1mix	AHSQVKFKLG DYLMFGPETRG	21	77.3	27.8	49.5	13	79.0	32.9	46.1	12
4_1L	L_{30}	30	110.4	40.0	70.4	19	112.8	44.0	68.8	18
4_1E	E_{30}	30	110.4	42.0	68.4	19	112.8	45.1	67.3	18
4_1G	G_{30}	30	110.4	50.0	60.4	16	112.8	63.0	49.8	13
4_1mix	TKGMLALYNS LSEEGKKDFQ AAYSASYYPS	30	110.4	38.7	71.7	19	112.8	44.3	68.5	18

TABLE I: Simulated knotted peptide systems. The peptides have $N_{\rm aa}$ amino acids (aa) with shown sequence. $l_{\rm c}$ is the estimated contour length of the unknotted peptide, l the measured end-to-end distance of the knotted peptide, and Δl the tight knot length involving $n_{\rm aa}$ amino acids. The lengths are evaluated at a stretching force of F_1=200 pN and F_2=1 nN.

FIG. 1: MD simulation snapshots of different protein knots in a 'cartoon' representation. a) Initial configuration of peptide 3_1G, where $l \simeq 25$ Å is the end-to-end distance. b) Tight knot configuration of peptide 3_1G. The end-to-end distance is $l \simeq 45.0$ Å at a stretching force $F \simeq 1.5$ nN. c) A tight 'figure-eight' knot configuration of peptide 4_1G at $F \sim 1$ nN. d) A tight 'pretzel' knot configuration of peptide 4_1L at $F \simeq 1$ nN.

FIG. 2: a) Force (F)-extension (l) curves for the peptides 3_1E, 3_1G, and 4_1L. Stretching curves (solid black lines) and loosening curves (dashed red lines) lie on top of each other indicating a small hysteresis. Pulling rate is 0.1 Å/ns. The inset shows the mean distance $\Delta l_{\rm aa}$ between neighboring backbone nitrogen atoms vs. stretching force F in an unknotted peptide. b) Force-extension curves for the polyleucine 3_1L. Black lines correspond to stretching while red lines correspond to loosening of the knot. While stretching, for extensions $l \lesssim 30$ Å a single water molecule is permanently trapped by the polar backbone of the peptide knot, see left snapshot. When exceeding $\simeq 30$ Å the water molecule is squeezed out (right snapshot) giving rise to a significant peak in the force-extension stretching curve. This transition leads to a considerable hysteresis when stretching and loosening curves are compared. The effect is reproducible when the stretching-loosening loop is repeated (dashed lines).

FIG. 3: MD simulation snapshots of the tightly knotted 4_1G (a) and 4_1mix (b). The backbone is sketched in a yellow ribbon for better identification and all amino acids are resolved in a 'licorice' representation ($F \simeq 1$ nN).

FIG. 4: Cowboy rope trick from B. S. Mason's book [53] showing a 4_1-knot with a 'pretzel'-like structure (left) and a 'figure-of-eight' structure (right). Fascinatingly, we find that both configurations are stable in proteins microscopica lly and depending on protein sequence. The book says instructively "The figure-of-eight is tied by precisely the same movements as t he pretzel. The factor determining which knot will result is the way the knot is dropped after shaking the rope off your arm. Jerk it as it falls and you should have the figure-of-eight. Shake it off gently and the pretzel should result." (Taken from http://www.inqui ry.net/outdoor/spin_rope/trick_knots.htm.)

FIG. 5: MD simulation snapshots of water trapped in peptide 4_1E (a) and 4_1mix (b) at a force $F \simeq 1$ nN. The backbone is shown in ribbon structure and only those residues are sketched ('licorice' representation) which are actively involved in water binding. Water (red and white spheres) is hydrogen bonded to the backbone amides. c) MD snapshot of 4_1mix in an unconstrained MD simulation. Four long-lived hydrogen bonds between backbone amides at the knot's ends are explicitly drawn (dotted blue lines).

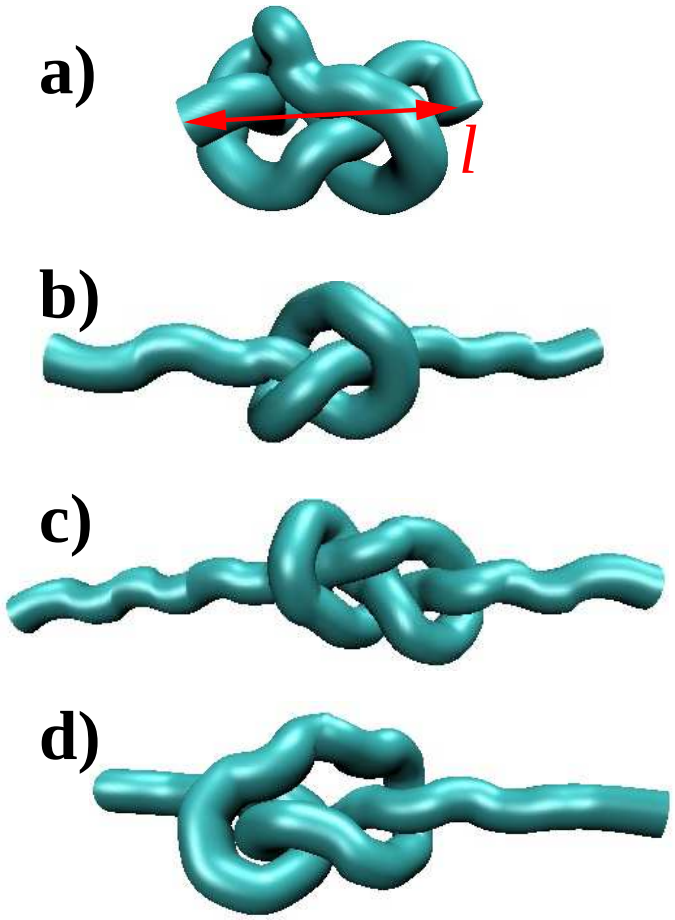


Fig. 1

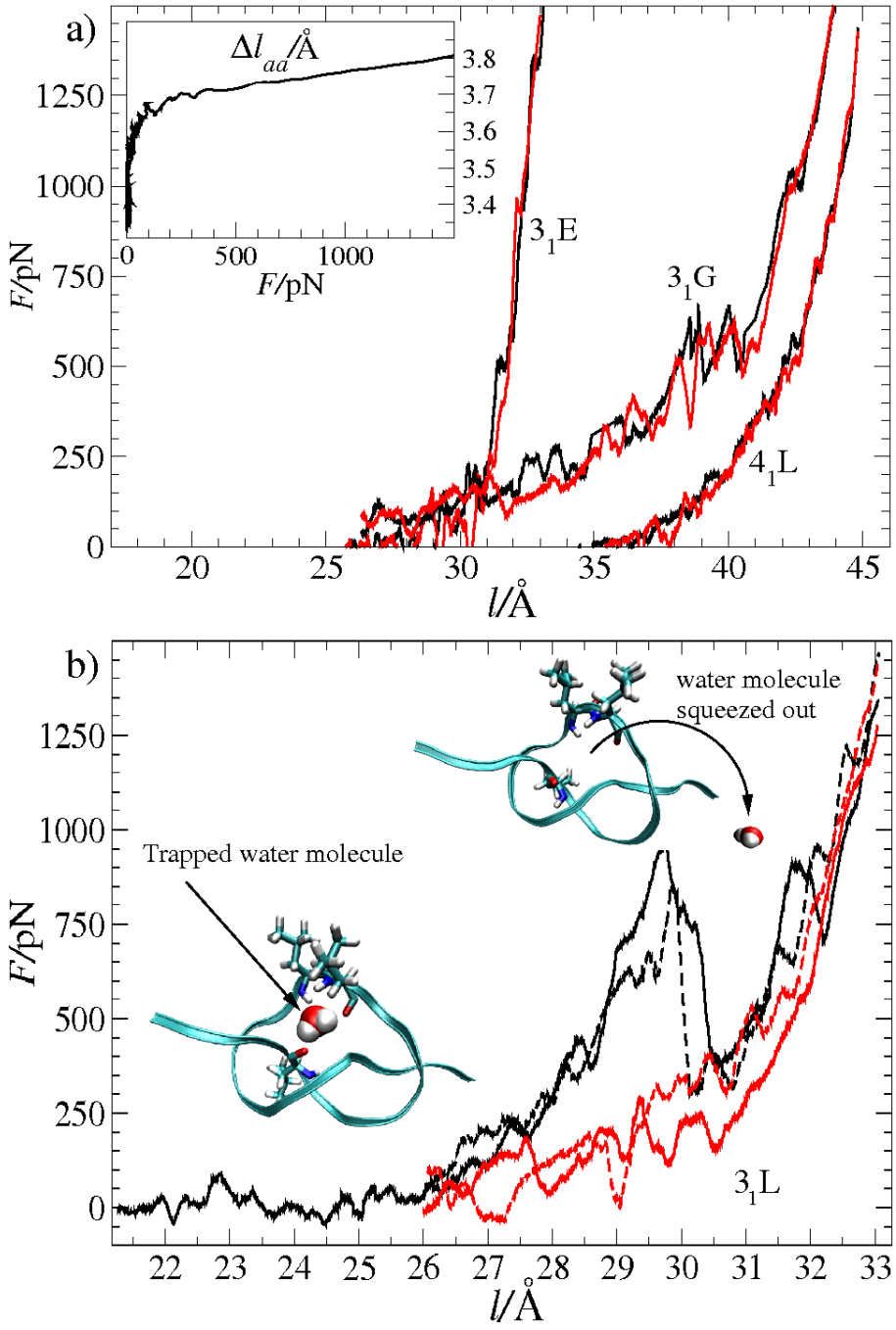

a)
Δl_{aa}/Å
3.8
3.7
3.6
3.5
3.4
0
500
1000
F/pN
1250
1000
750
500
250
0
F/pN
3_1E
3_1G
4_1L
20
25
30
35
40
45
l/Å
b)
water molecule
squeezed out
Trapped water molecule
1250
1000
750
500
250
0
F/pN
3_1L
22
23
24
25
26
27
28
29
30
31
32
33
l/Å

Fig. 2

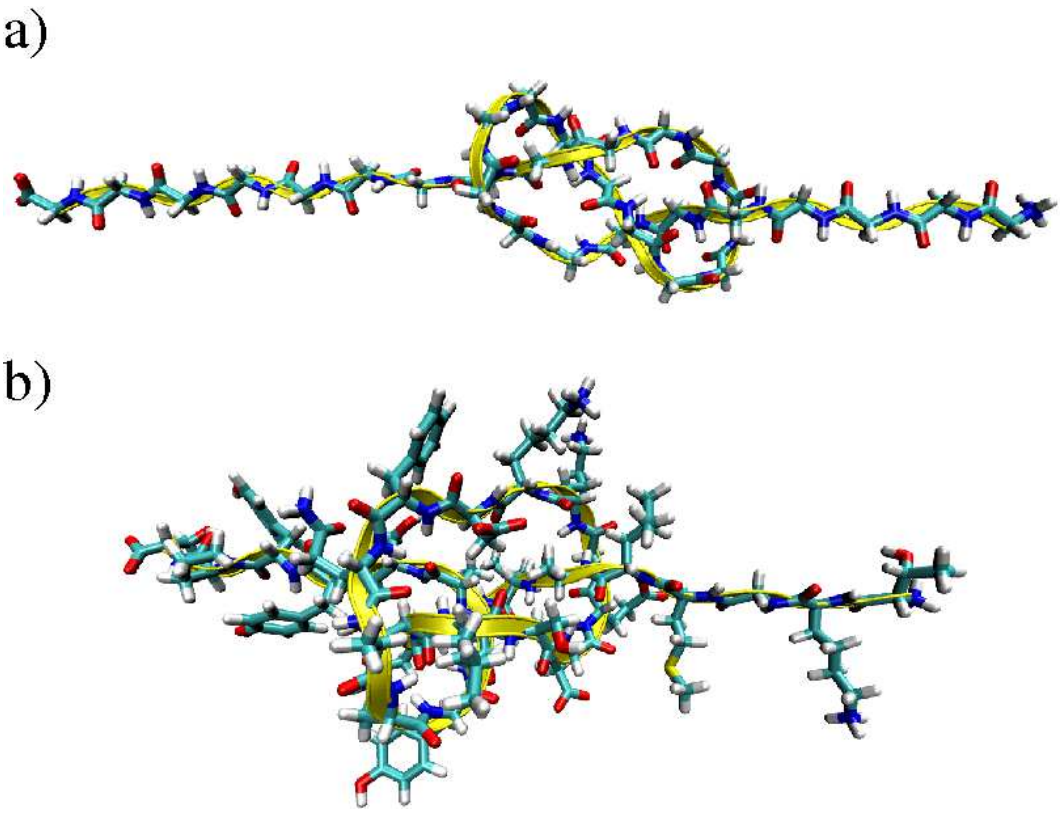
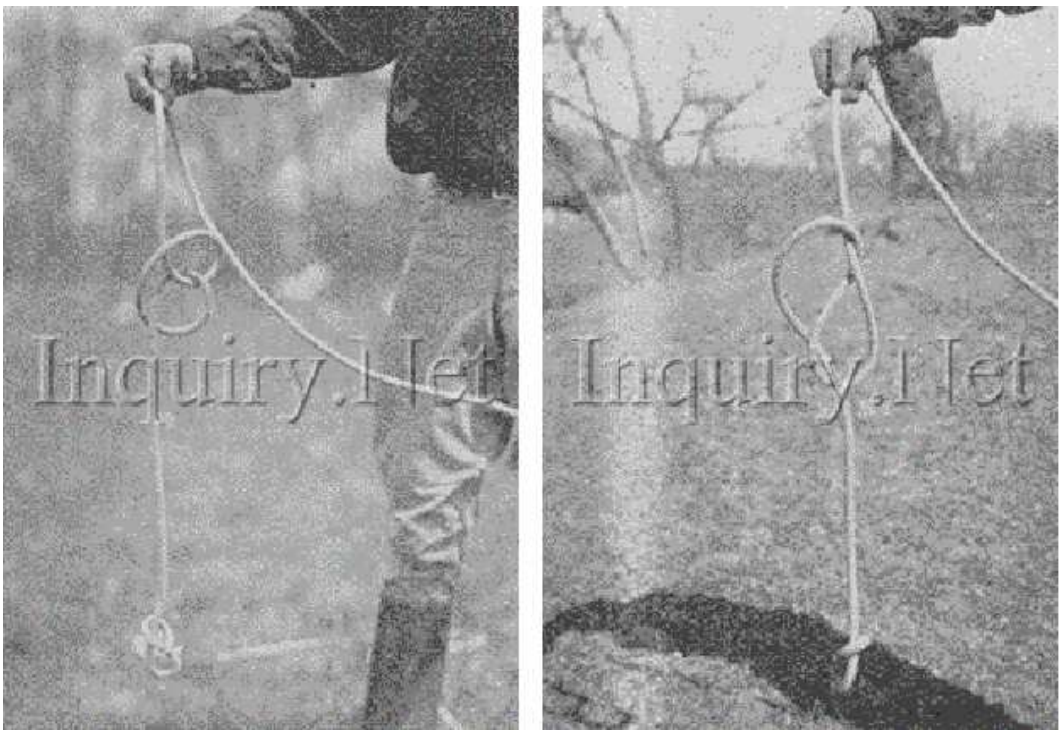


Fig. 3

Fig. 4 

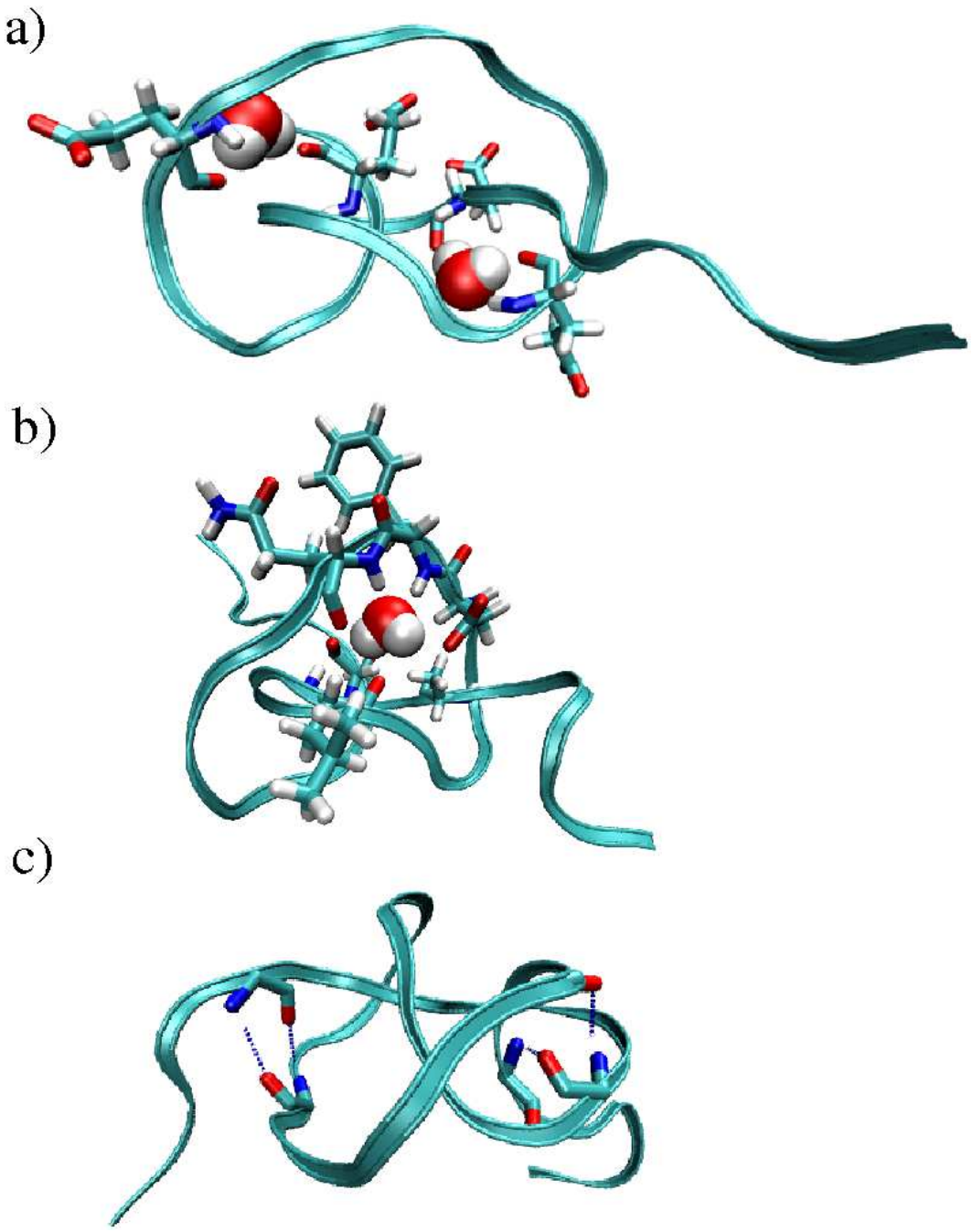


Fig. 5